

Influence of compacting pressure on the electrical properties of ZnO and ZnO:Mn ceramics

N. Korsunskaya¹ · I. Markevich¹ · T. Stara¹ · Yu. Polishchuk¹ · S. Ponomaryov¹ · K. Kozoriz¹ · Z. Tsybrii¹ · O. Melnichuk² · L. Melnichuk² · E. Venger¹ · L. Khomenkova^{1,3}

Received: 1 December 2023 / Accepted: 6 February 2024

Published online: 16 February 2024

© The Author(s) 2024 [OPEN](#)

Abstract

Undoped and Mn-doped ZnO ceramics were prepared from the powders compacted at different pressures and sintered in air at high temperature. Their structural, optical, light emitting and electrical characteristics as well as the distribution of chemical elements were studied. It was found that an increase in compacting pressure stimulates an increase in direct current conductivity in both undoped and doped samples. In the case of doped samples, this effect was accompanied by a decrease in the height of potential barriers at the grain boundaries. It is found that electron concentration in ceramic grains, estimated from the modelling of infrared reflection spectra, remained relatively constant. The analysis of luminescence spectra and spatial zinc distribution revealed that the increase in compacting pressure results in the accumulation of interstitial zinc at the grain boundaries forming channels with enhanced conductivity. These findings provide an explanation for the evolution of electrical properties of ceramic samples with compacting pressure.

Article Highlights

- ZnO and ZnO:Mn powders compacted with different pressure were sintered in air.
- The rise of compacting pressure enhances electrical conductivity of the ceramics.
- Compacting pressure decreases the superlinearity of I-V curves in ZnO:Mn.
- The formation of conductive channels was observed in both ZnO and ZnO:Mn.
- Zinc accumulation at grain boundaries favours conductive channels formation.

Keywords ZnO · Manganese · Doping · Ceramics · Electrical properties · Grain boundaries · Segregation · XRD · Auger spectroscopy · Scanning electron microscopy · Infrared reflection spectroscopy

1 Introduction

Intrinsic defects such as vacancies, interstitial atoms and antisite defects are typically present in the crystal lattice, exerting a significant impact on the functionality of semiconductor materials. The effective management of intrinsic defects in semiconductors is crucial for their successful industrial applications.

✉ L. Khomenkova, khomen@ukr.net | ¹V. Lashkaryov Institute of Semiconductor Physics of National Academy of Sciences of Ukraine, 45, Pr. Nauky, Kyiv 03028, Ukraine. ²Nizhyn Mykola Gogol State University, 2 Hrafska Str., Nizhyn 16600, Ukraine. ³National University "Kyiv Mohyla Academy", 2 Skovorody Str., Kyiv 04070, Ukraine.



Zinc oxide (ZnO) is an important wide bandgap oxide semiconductor used in various applications, including sensors, varistors, transparent electrodes, and light-emitting devices. Additionally, the combination of ferromagnetic and semiconductor properties of ZnO facilitates the development of modern spintronic devices.

To enhance the properties of zinc oxide and broaden its range of applications, researchers often turn to doping ZnO. Among the various impurities investigated, manganese is one of the most studied in ZnO. The exactly half-filled 3d-orbitals of manganese facilitate its incorporation into ZnO lattice, playing a crucial role in improving the characteristics of ZnO-based varistors [1, 2]. High-temperature ferromagnetism has been reported for Mn-doped ZnO films, powders and pellets [3, 4]. It was observed that the incorporation of manganese into lattice sites, coupled with oxygen vacancy formation [5, 6], contributed to the appearance of ferromagnetism. At the same time, the presence of zinc vacancies (V_{Zn}) in Mn-doped ZnO films was considered as the factor that induced ferromagnetic ordering [7].

The electrical and luminescent properties of ZnO are known to be highly dependent on the presence of nonstoichiometric intrinsic defects. The most important of them are interstitial zinc ions (Zn_i) that determines the conductivity of ZnO. As it was shown earlier [8–10], Zn_i is a mobile defect which can lead to its spatial redistribution in the crystal. In particular, the drift of Zn_i in the surface band bending due to oxygen adsorption leads to its accumulation in the near-surface region of crystals [9]. These defects also decorate dislocations [10], which influences the shape of the bandedge luminescence. Additionally, Zn_i is also a component of the complex responsible for the green self-activated luminescence band and can drift in the external electric field at 200–300 °C [8]. On the other hand, the distribution of Zn_i can be influenced by the pressure applied to ZnO crystal. More specifically, the application of pressure can lead not only to the transformation of the hexagonal phase of ZnO into cubic one but also to the extraction of Zn_i from ZnO lattice, resulting in the formation of hexagonal metallic zinc [11]. Consequently, both the content of intrinsic Zn_i defects and their spatial distribution depend on the approach used for the materials production and their subsequent thermal treatments.

It should be noted that compaction is usually applied to form ZnO-based ceramics that are widely used as varistors, phosphors with long afterglow, catalysts, gas sensors, etc. Regarding varistors, their production is, at least, a two-stage process. In the first stage, the raw powders are grounded and then they are compacted to achieve the required shape. It is worth pointing out that in most research, the effect of applied pressure on the characteristics of ready-made varistors was investigated only. Specifically, it was shown that the increase of applied pressure (in the range of 10–200 MPa) results in the increase of the current and the reduction of the slope of the current–voltage (I–V) characteristics due to barrier lowering [12–14]. This effect has been suggested to be caused by the influence of piezo-fields [15]. In some works, the elimination of pressure led to the restoration of the original characteristics [12], while in others [13] a residual effect was observed. However, its origin has not been reported in those studies.

As for the impact of pressure in the manufacture of ceramic samples, only the effect of grinding the raw powders was studied. For instance, it has been shown [16] that it leads to zinc enrichment of ceramic grain boundaries. Since interstitial zinc ions (Zn_i) play a crucial role in ZnO conductivity [17, 18], the spatial redistribution of these defects can significantly influence the electrical properties of ceramics and can be one of the factors that determine the characteristics of devices. Specifically, this can be essential for ceramics used as varistors or gas sensors. Thus, the investigation of defect redistribution, including under pressure, can be required.

At the same time, the effect of powder compacting on ceramic electrical conductivity (that is important characteristic for varistors and gas sensors) as well as on luminescence intensity has not been studied. Therefore, in this work, the investigation of structural, electric and luminescent characteristics, as well as microscopic chemical analysis of undoped and manganese-doped ZnO ceramic samples versus the pressure applied upon the compacting of the corresponding powders was carried out.

2 Experimental details

Undoped ZnO ceramic samples were prepared using commercial ZnO powders (99.99% purity) mixed with distilled water. For Mn-doped ZnO samples, the ZnO powder was mixed with $MnSO_4$ aqueous solution. The manganese content in the charge was fixed at 0.1 at.% because this doping level is known to be used in the manufacture of ZnO-based varistors to increase the slope of their current–voltage characteristics [1, 2]. Manganese was present as a substitution ion Mn_{Zn}^{2+} while no other defects were registered.

For “unpressed” ZnO and ZnO:Mn ceramics ($P = 0$ MPa), corresponding wet mixtures were hand-prepared in the shape of rectangle parallelepipeds. To create compacted samples, the same powder mixtures were air-dried at room temperature for 3 days to eliminate water excess. Compaction was carried out at the pressures ranging from 25 to 150 MPa for 30 min using rectangle mold. It is important to note that these pressure values are usually used in the varistor

manufacturing. After compaction, the specimens were placed in a muffle furnace and heated up to $T = 1050\text{ }^{\circ}\text{C}$ with a ramp of $\sim 400\text{ }^{\circ}\text{C/h}$ in air atmosphere. This was followed by sintering for 3 h at this temperature, and then the specimens were gradually cooled down to room temperature with the furnace.

The structural, optical, luminescent, and electrical characteristics of the ceramic samples were thoroughly investigated using multiple techniques. X-ray diffraction (XRD) analysis was conducted in Bragg–Brentano geometry (Θ – 2Θ) with $\text{Cu}_{K\alpha 1}$ radiation, employing a Philips X'Pert-MRD diffractometer. Scanning electron microscopy (SEM) images and Auger maps were obtained with a JAMP-9500F (JEOL) tool equipped with an Auger microprobe, featuring a spatial resolution of 3 nm in the secondary electron image mode. The microprobe included a sensitive hemispheric Auger spectrometer with energy resolution ($\Delta E/E$) ranging from 0.05 to 0.6% and an ion etching gun for layer-by-layer analysis. For chemical maps, a preliminary etching process with Ar ions was employed to remove approximately a 100-nm surface layer and clean the samples from contaminations. The Ar^+ ion beam had a diameter of 120 μm , capable of rastering over a $1 \times 1\text{ mm}^2$ area. The beam's Ar + ion energy ranged from 0.01 to 4 keV, with a minimal beam current of 2 μA at 3 keV.

Additionally, infrared reflection spectroscopy, photoluminescence (PL), and direct current (DC) methods were employed. Specular infrared reflection spectra were obtained from polished samples using a Spectrum BX spectrometer (PerkinElmer Inc.). The incident angle of the excitation light was 13° , and a gold mirror served as a reference. Spectra were recorded with a resolution of 1 cm^{-1} . Photoluminescence (PL) spectra were excited using a nitrogen laser (337.1 nm) and recorded with a Concave BlackCommet spectrometer (StellarNet Inc., USA) in the spectral range of 340–750 nm. For electrical characterization, the samples were cut transversally, and indium ohmic contacts were deposited on the cleft surfaces. Current–voltage characteristics and the temperature dependence of the conductivity were then measured.

3 Results and discussion

3.1 XRD and SEM study

Figure 1a displays XRD patterns of undoped ZnO ceramics. All XRD peaks correspond to hexagonal ZnO and the ratio of their intensities does not show the predominant orientation of ZnO crystallites (according to the ICDD Card No. 010-70-8072). Analysis of XRD patterns for the samples compacted with $P = 25$ – 150 MPa revealed no significant variation of the XRD peak positions and their full-width at half-maximum as well as the ratio of their magnitudes (Fig. 1a, b). The ratio of the amplitudes and the positions of XRD peaks of Mn-doped samples were found to be similar to those of undoped samples. This indicates that there is no preferred orientation of ZnO crystallites in all samples. Furthermore, no noticeable residual stresses are observed in ZnO and ZnO:Mn ceramics.

Figure 1c and d demonstrate that an increase in compacting pressure results in a decrease of ceramic porosity and an increase in grain sizes. Besides, for Mn-doped ZnO samples, no additional phases, including Mn-related ones, were detected. These results show that compacting does not affect the orientation of the crystallites and does not create noticeable residual stresses in Mn-doped ZnO all samples. The SEM observation revealed that the structure of Mn-doped samples was similar to that of undoped ZnO ones and the increase in compacting pressure results also in the decrease of ceramic porosity and in the increase of grain sizes.

3.2 DC conductivity

In both undoped and doped ZnO samples, an increase in the value of DC conductivity was observed with increasing pressure. However, other characteristics, particularly current–voltage relationships and temperature dependence of DC conductivity, exhibited differences.

The current–voltage characteristic for the undoped sample formed at $P = 0\text{ MPa}$ is shown in Fig. 2a. Because of high sample conductivity at room temperature, it was measured at 77 K. It demonstrated linearity, a typical feature of undoped ZnO ceramics originating from the absence of the barriers between the grains [19]. The DC conductivity of this sample at 300 K is $\sigma \sim 3 \times 10^{-3}\text{ Ohm}^{-1}\text{ cm}^{-1}$ being closed to that for $P = 25\text{ MPa}$. Simultaneously, the increase in pressing pressure causes a rise in conductivity, reaching $\sigma \sim 5 \times 10^{-2}\text{ Ohm}^{-1}\text{ cm}^{-1}$ at 300 K for $P = 150\text{ MPa}$, i.e. higher by approximately 10 times.

The increase in compacting pressure also induced a modification in the temperature dependence of DC conductivity (Fig. 2b). It is evident that in undoped ZnO samples, compacted with $P = 25$ and 50 MPa , the conductivity decreases

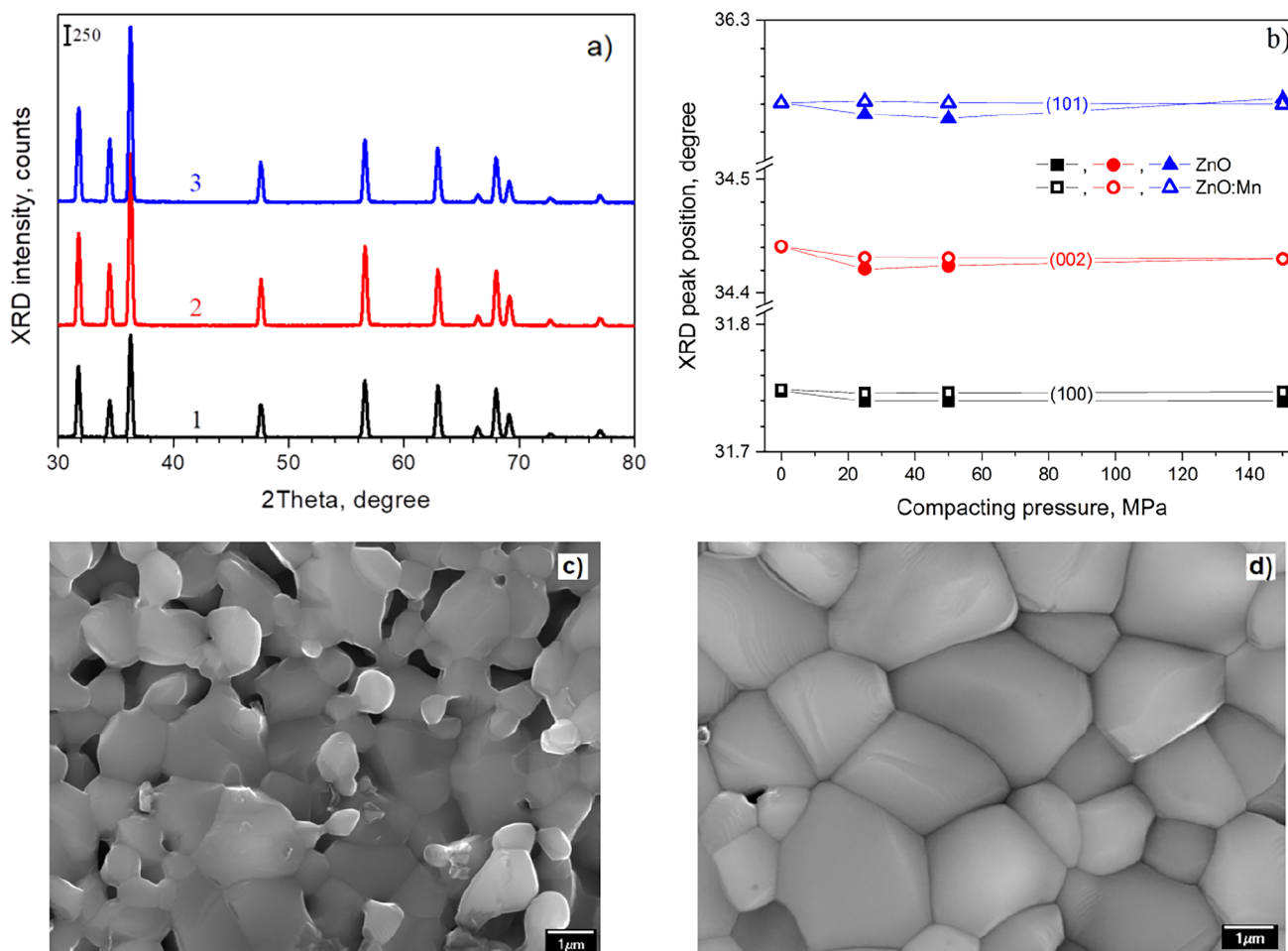


Fig. 1 **a** XRD patterns of ZnO samples compacted at P=0 (1), 50 (2) and 150 (3) MPa; **b** the variation of the positions of (100), (002) and (101) XRD peaks for ZnO and ZnO:Mn samples versus compacting pressure; **c**, **d** SEM images of the surface of ZnO ceramics compacted with P=25 (c) and 150 (d) MPa

with decreasing temperature due to the filling of shallow donors. Conversely, in the sample made with P = 150 MPa, the temperature dependence of the DC conductivity is almost absent.

Unpressed ZnO:Mn samples, in contrast to undoped counterparts, exhibit higher resistivity at room temperature ($\sigma \sim 10^{-5} \Omega^{-1} \text{cm}^{-1}$) and their current–voltage characteristics are superlinear (Fig. 3). This superlinearity is known to result from the formation of barriers at the grain boundaries [20]. In these samples, an increase in the conductivity value with increasing pressure was also observed, accompanied by a decrease in the slope of the current–voltage characteristics. Finally, at P = 150 MPa, the current–voltage characteristics became almost linear (Fig. 3). The slope of the temperature dependence of DC conductivity also decreased (Fig. 3), but even at P = 150 MPa, this dependence did not vanish.

In general, the conductivity increase may be attributed to several factors, including the decrease in barrier height, an increase in the concentration of electrons in ceramic grains, a reduction in the number of pores, and the formation of specific conductive channels that bypass grains. In the latter case, the temperature dependence of DC conductivity may be absent.

The presence of barriers in ceramics can be indicated by the superlinearity of the current–voltage characteristics. As mentioned above, they are linear in undoped samples, confirming the absence of barriers in these ZnO ceramics. This aligns with the findings reported in Refs. [21, 22]. In the case of ZnO:Mn samples, their current–voltage characteristics indeed showed superlinearity. However, with an increase in compacting pressure, the degree of superlinearity decreased, and eventually, the current–voltage characteristics became almost linear. Thus, it can be concluded that the increase in DC conductivity in undoped samples was not caused by a change in the height of the barriers, whereas this effect may occur in doped samples.

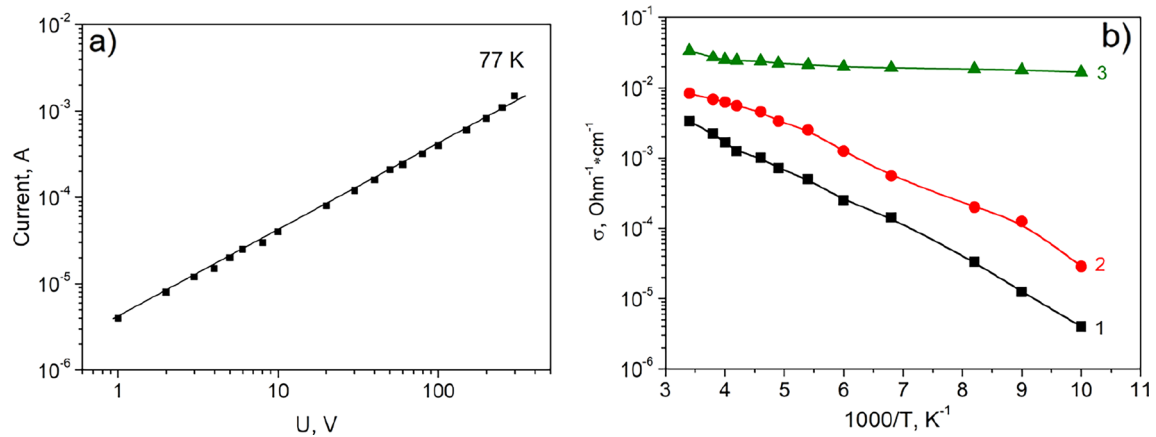


Fig. 2 **a** Current–voltage characteristic measured at 77 K for undoped ZnO sample formed without pressing ($P=0$ MPa). **b** Temperature dependences of DC conductivity for ZnO samples compacted with $P=25$ (1), 50 (2) and 150 (3) MPa. $U=10$ V

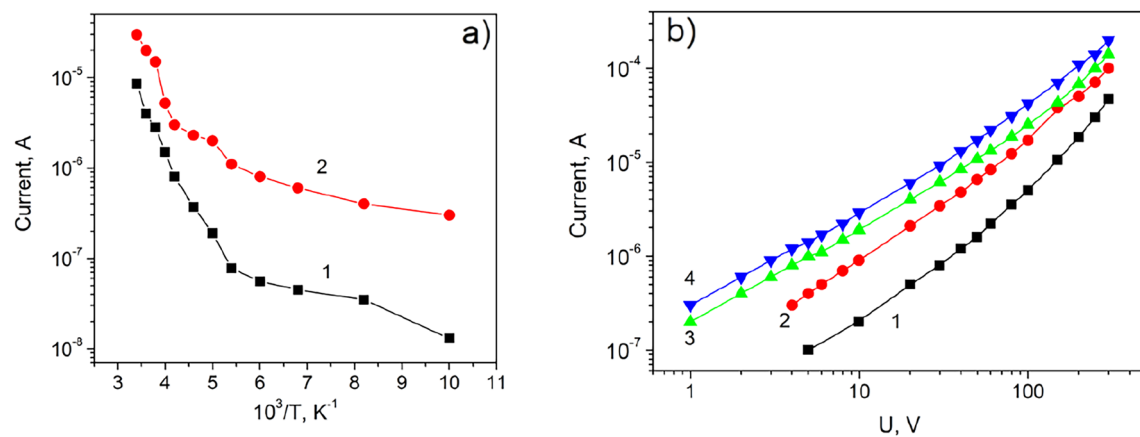


Fig. 3 **a** Temperature dependence of conductivity of ZnO:Mn samples compacted with $P=25$ MPa (1) and 150 MPa (2); **b** room temperature current–voltage characteristics for ZnO:Mn samples compacted with $P=0$ (1), 25 (2), 50 (3) and 150 (4) MPa

3.3 IR reflection spectra

To assess the impact of pressure on the concentration of electrons in ceramic grains, modeling of IR reflection spectra was conducted for the same samples, considering the contribution of the plasma subsystem. The IR reflection spectra were found to be similar for undoped and Mn-doped samples compacted with the same P value. Therefore, in Fig. 4, the effect of pressure is demonstrated for undoped samples only.

To fit the experimental data, the approach described in Refs. [23–25] was used. The parameters for the orientation of electric field component $\mathbf{E} \perp \mathbf{C}$ were taken as $\nu_{\text{TO1}}=412 \text{ cm}^{-1}$, $\nu_{\text{LO1}}=585 \text{ cm}^{-1}$, $\epsilon_0=3.95$ and $\epsilon_\infty=8.1$. For the case $\mathbf{E} \parallel \mathbf{C}$, the fitting was performed with $\nu_{\text{TO1}}=390 \text{ cm}^{-1}$, $\nu_{\text{LO1}}=570 \text{ cm}^{-1}$, $\epsilon_0=4.05$ and $\epsilon_\infty=9.0$. The frequency dependence of the dielectric constant was considered as a function with additive and phenomenological contribution of phonon and plasmon subsystems. This approach allowed the determination of carrier concentration, mobility, and the conductivity of ceramic grains. The results of the fitting of the spectra, presented in Fig. 4, are summarized in Table 1.

As can be seen from Table 1, the concentration of electrons in the grains of undoped ceramics, as well as the conductivity value of the ZnO grains estimated from the IR reflection spectra (Fig. 4), change only slightly with increasing pressure. Meanwhile, the DC conductivity increases by more than 10 times. Therefore, it can be concluded that the increase in DC conductivity of undoped ceramics with increasing compacting pressure is not caused by the changes in grain conductivity.

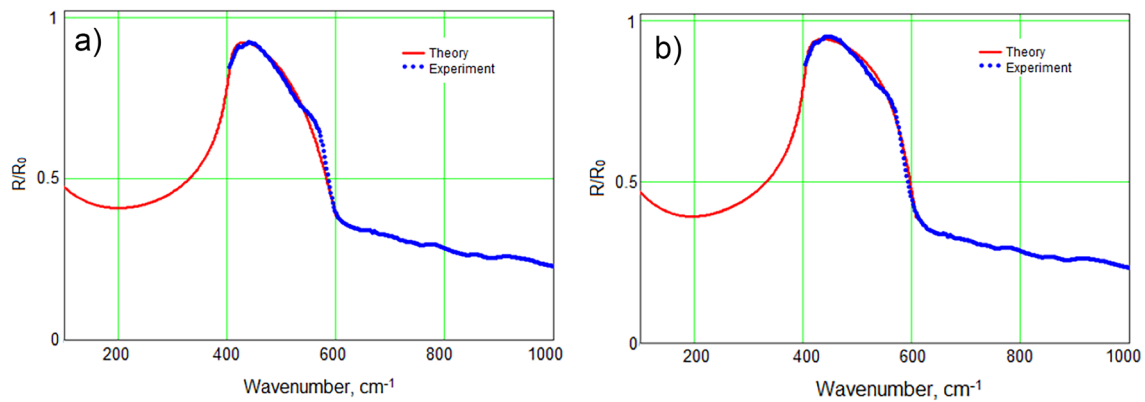


Fig. 4 Experimental (symbols) and simulated (solid curves) IR reflection spectra for undoped ZnO ceramics obtained at compacting pressures of 25 (a) and 150 (b) MPa

Table 1 The electrophysical and optical parameters of ZnO ceramics compacted at different pressures

Parameter	ZnO samples compacted with different pressure		
	P=0 MPa	P=25 MPa	P=150 MPa
ν_p , cm^{-1}	270	380	300
γ_p , cm^{-1}	800	620	380
γ_{TO} , cm^{-1}	100	12	10
γ_{LO} , cm^{-1}	50	24	10
Carrier concentration, n_0 , cm^{-3}	1.0×10^{18}	1.67×10^{18}	1.04×10^{18}
Conductivity of grains, σ , $\Omega^{-1} \text{cm}^{-1}$	44,8	96,1	97,7
Mobility μ , $\text{cm}^2/(\text{Vs})$	28,0	36,1	57,9

It should be noted that doping with Mn does not alter the grain conductivity [19], as the energy level of $\text{Mn}_{\text{Zn}}^{2+}$ cations is deep and lies below Fermi level. However, their presence in ceramics stimulates the formation of barriers at the grain boundary, resulting in a decrease in its DC conductivity.

Another reason for the increase in DC conductivity due to compacting may be a reduction in porosity with increasing pressure. In this case, its temperature dependence should not change significantly. This scenario can be realized for $P=50$ MPa. However, at $P=150$ MPa, the temperature dependence of DC conductivity is almost absent. Therefore, we can assume that, in this case, the main reason for the increase in DC conductivity is evidently the formation of conductive channels. It is worth nothing that this may initially lead to a decrease in the slope of the temperature dependence of DC conductivity. Then, with an increase in channel conductivity, it eventually disappears (if channel conductivity is temperature-independent). This situation is observed in the experiment (Fig. 2).

It should be noted that the increase in pressure and the formation of channels do not change practically the carrier content in the grains (changes within experimental error). Since Zn interstitials are the main donors responsible for ZnO conductivity, this may indicate that the quantity of zinc accumulated at the grain boundaries (forming channels) does not significantly change the concentration of Zn interstitials in the grains.

For Mn-doped ZnO, no effect of manganese on the concentration of free electrons in ceramic grains is found, and as in the case of undoped samples, it is independent of pressure value. Thus, even in doped samples, the increase in DC conductivity value with increasing compacting pressure is not associated with a change in the conductivity of ceramic grains.

At the same time, as seen from Fig. 3, the slope of the current–voltage characteristics in these samples decreases, and at the pressure of $P=150$ MPa, they become almost linear, indicating a decrease in the effect of barriers on DC conductivity.

Therefore, the decrease in the height of the barriers at the grain boundaries can be considered as one of the reasons for the increase in DC conductivity of doped samples. However, the decrease in the slope of the temperature dependence of the conductivity with increasing pressure value may also indicate the formation of conductive channels. In this case, their effect may increase with decreasing temperature due to a decrease in the grain conductivity, and at low temperatures, channel conductivity may exceed grain conductivity. This may explain the greater change in conductivity at low temperatures

with increasing compacting pressure. Thus, manganese-doped samples are likely have two reasons for the increase in DC conductivity with compacting pressure, namely, the decrease in barrier height and the appearance of conductive channels.

Because the barriers are due to the formation of a depletion layer near the grain boundaries due to oxygen adsorption, a decrease in their height in ceramic samples can be caused by an increase in carrier concentration near the grain boundaries.

3.4 Photoluminescence spectra

Some information on the nature of the conductive channels can be obtained from the analysis of photoluminescence spectra. As seen from Fig. 5, the PL spectrum includes emission of free exciton and its phonon replica, as well as a broad defect-related band that contains several components: 510 nm (~ 2.43 eV), 530–550 nm (2.34–2.25 eV), and 580 nm (~ 2.14 eV). It has been found that the increase in compacting pressure leads to an enhancement of the exciton emission and to a decrease in the intensity of the defect-related bands, the contribution of the component of 510 nm (~ 2.43 eV) mainly reduced. As shown in Ref. [8], the latter band originates from a complex including interstitial zinc (Zn_i). It should be noted that a similar change in the ratio of the intensity of the luminescence bands was observed in Ref. [26] when the surface of the ceramic sample was mechanically disturbed due to scratches with a sharp metal tip.

The decrease in the intensity of the green band indicates a reduction in the concentration of Zn_i in the whole grain or in some part of it. It is essential that a partial depletion of grains may not significantly affect the plasmon frequency and, accordingly, the electron concentration estimated from the IR reflection spectra. Indeed, the plasmon frequency is

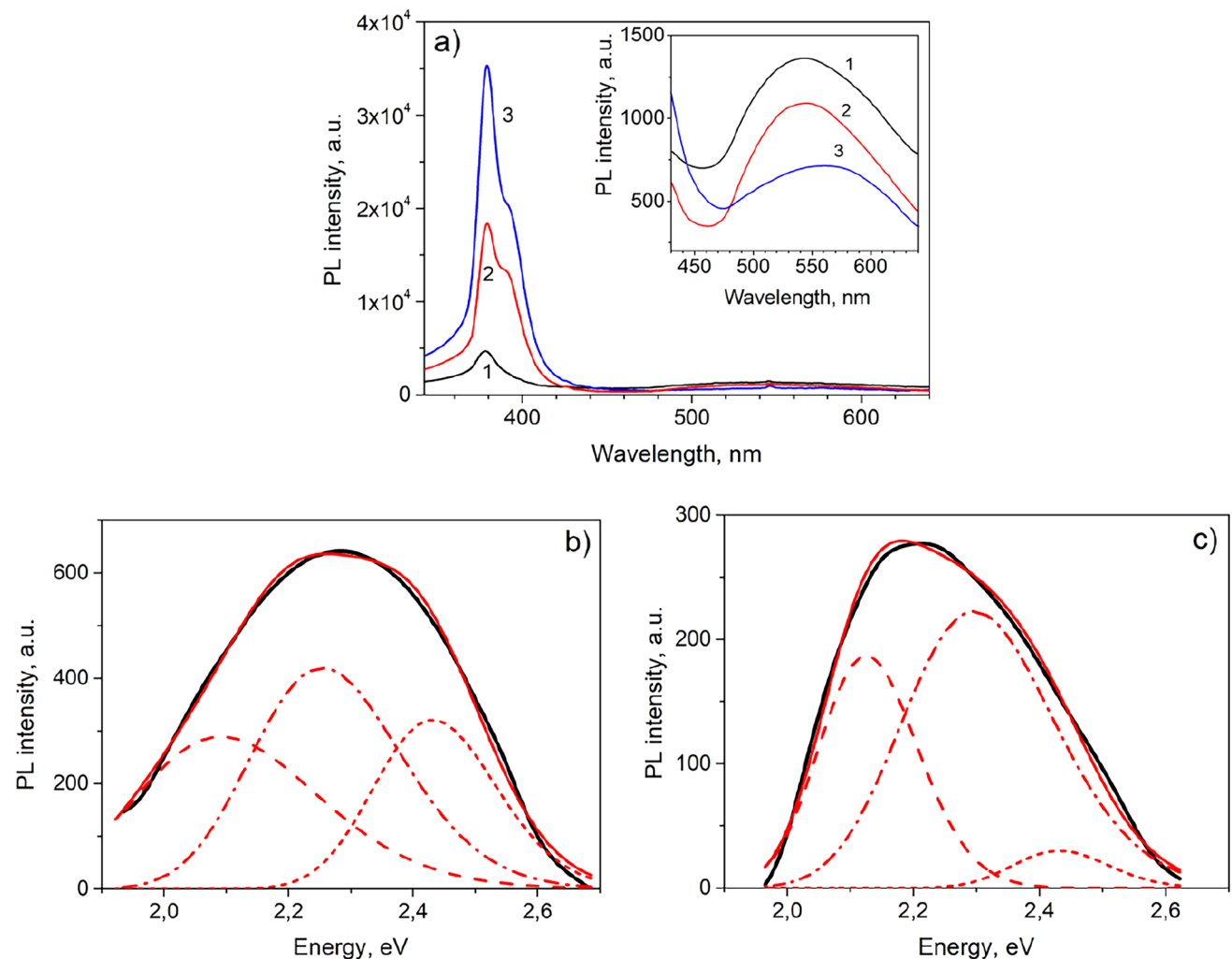


Fig. 5 **a** Photoluminescence spectra of undoped ZnO samples, pressed at $P=25$ (1), 50 (2) and 150 (3) MPa. The inset shows in details the defect-related PL band; **b**, **c** the decomposition of the defect-related bands presented in **(a)** on PL components for curve 2 **(b)** and curve 3 **(c)**

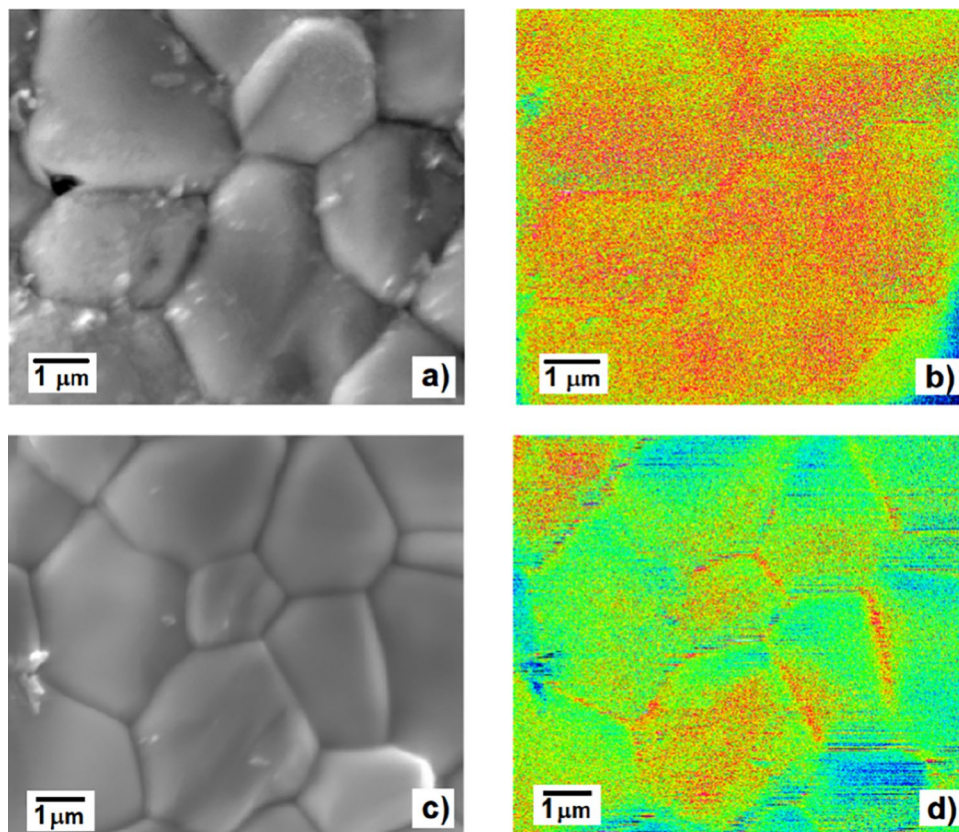
primarily determined by the contribution of the grain part with a higher electron concentration, and the areas depleted of Zn_i may not significantly affect the electron concentration estimated from the IR reflection spectra. This aligns with our observation.

Thus, it can be concluded that increasing the compacting pressure leads to a decrease in the content of Zn_i in some part of the ceramic grain. Simultaneously, Zn_i can accumulate in some other areas of the ceramic sample, which act as channels with high conductivity. The latter may be dislocations that can form during compacting or grain boundaries. Notably, the accumulation of Zn interstitials near dislocations was observed in ZnO single crystals [10], while the appearance of metal zinc on the surface of nanocrystals after the application of hydrostatic pressure of several GPa was found in Ref. [11].

It is noteworthy that the accumulation of Zn_i near the dislocations results usually in a decrease in the intensity of the phonon-free line compared to its phonon replica in the exciton emission spectrum. This phenomenon was not observed in our case. Therefore, we can infer that the formation of conductive channels is primarily attributed to the accumulation of Zn_i at the grain boundaries. This deduction is substantiated by the Auger maps (Fig. 6), which depict the surface image and spatial distribution of zinc for ZnO samples compacted at $P=50$ MPa (Fig. 6a, b) and 150 MPa (Fig. 6c, d). In these presentations, the green color corresponds to a lower Zn content, while the red color indicates a higher amount. A comparative analysis of SEM COMPO images of the ceramic surfaces with corresponding distribution of the intensity of Zn-related Auger signal reveals that the grain boundaries are enriched in zinc. Furthermore, the gradient in Zn content in ZnO sample compacted at 150 MPa is more pronounced than that in the sample prepared at 50 MPa.

It is seen that the increase of compacting pressure (Fig. 6a) results in the decrease of ceramic porosity which is significant at $P=25$ MPa but is low enough for $P=50$ and 150 MPa. At the same time, Zn-related Auger maps for $P=50$ MPa and $P=150$ MPa show the increased Zn content at grain boundaries (Fig. 6b). Thus, the main reason of conductivity increase is the formation of conductive channels due to Zn accumulation on the grain boundaries. The more pronounced effect was found for the ZnO compacted with $P=150$ MPa (Fig. 6d). This testifies to the enhancement of grain boundary Zn enrichment with increase of compacting pressure. One of the possible reasons of Zn accumulation at the grain boundaries can be Zn extraction from the grains facilitated by appearance of electric field due to piezo effect.

Fig. 6 SEM COMPO images of ceramic morphology (a, c) and Zn-related Auger maps (b, d) for ZnO samples compacted at $P=50$ MPa (a, b) and 150 MPa (c, d). The Auger maps are qualitative. The green color corresponds to the lower Zn amount and the red—to the higher Zn amount. The maps show that the gradient in Zn content in image (d) is more prominent than that in image (b)



4 Conclusion

The impact of compacting pressure on the structural, luminescent, and electrophysical characteristics of undoped and manganese-doped ZnO ceramics was investigated by X-ray diffraction, IR reflection spectroscopy, photoluminescence, and DC electrical conductivity, along with SEM and Auger spectroscopy methods. It was observed that compacting pressure does not influence the orientation of the ZnO crystallites and does not create significant residual stresses. However, it brings substantial changes in electrical and luminescent characteristics. The increase in compacting pressure results in enhanced DC conductivity of undoped ceramics, and at a pressure of 150 MPa, the temperature dependence of its conductivity disappears. In doped samples, both an increase in DC conductivity and a reduction in the superlinearity of the current–voltage characteristics were observed.

Possible reasons of these changes are considered, including the increase in DC conductivity due to the decreased height of barriers at grain boundaries, enhanced electron concentration in ceramic grains, reduced porosity and the formation of highly conductive channels bypassing grains.

The comparison of electrophysical parameters obtained from DC measurements and modeling of IR reflection spectra demonstrated that an increase in compacting pressure does not significantly alter the concentration of electrons in ceramic grains. In undoped samples, the absence of barriers is inferred from the linearity of the current–voltage characteristics. The primary reason for observed conductivity increase is concluded to be the formation of channels with high conductivity bypassing ceramic grains. In doped samples, the decrease in the slope of current–voltage characteristics and the temperature dependence of DC conductivity can also be attributed to the formation of conductive channels. The analysis of the Zn-related Auger maps and luminescence spectra suggests that the increase in compacting pressure results in the accumulation of interstitial zinc at the grain boundaries acting as channels with enhanced conductivity. The formation of these channels may also contribute to a decrease in barrier height.

Acknowledgements This work was supported by the National Academy of Sciences of Ukraine as well as by the National Research Foundation of Ukraine from the state budget, project 2020.02/0380 «Structure transformation and non-equilibrium electron processes in wide bandgap metal oxides and their solid solutions». The authors appreciate the support from Springer Nature provided for Ukrainian researchers for the publication of this paper in open access mode.

Author contributions NK: Conceptualization, Writing—original draft, Writing—review and editing. IM: Conceptualization, Investigation, Writing—review and editing. TS: Investigation, Formal analysis, Visualization, Writing—review and editing. YP: Investigation, Formal analysis, Writing—review and editing. SP: Investigation, Formal analysis, Writing—review and editing. KK: Investigation. ZT: Investigation, Writing—review and editing. OM: Investigation, Formal analysis, Software, Writing—review and editing, Funding acquisition. LM: Investigation, Formal analysis, Software, Validation, Writing—review and editing. EV: Writing—review and editing, Funding acquisition. LK: Supervision, Investigation, Formal analysis, Visualization, Writing—review and editing.

Funding National Academy of Sciences of Ukraine (project III-4-21) and the National Research Foundation of Ukraine from the state budget, project 2020.02/0380 «Structure transformation and non-equilibrium electron processes in wide bandgap metal oxides and their solid solutions». Open access funding is provided by Springer Nature.

Data availability The raw/processed data required to reproduce these findings cannot be shared at this time as the data also forms part of an ongoing study.

Declarations

Ethics approval and consent to participate The authors declare that they have no potential conflicts of interest. Human participants and animals were not involved in this research.

Competing interests The authors have no competing interests to declare that are relevant to the content of this article. The authors have no relevant financial or non-financial interests to disclose.

Open Access This article is licensed under a Creative Commons Attribution 4.0 International License, which permits use, sharing, adaptation, distribution and reproduction in any medium or format, as long as you give appropriate credit to the original author(s) and the source, provide a link to the Creative Commons licence, and indicate if changes were made. The images or other third party material in this article are included in the article's Creative Commons licence, unless indicated otherwise in a credit line to the material. If material is not included in the article's Creative Commons licence and your intended use is not permitted by statutory regulation or exceeds the permitted use, you will need to obtain permission directly from the copyright holder. To view a copy of this licence, visit <http://creativecommons.org/licenses/by/4.0/>.

References

1. Han J, Senos AMR, Mantas PQ. Varistor behaviour in Mn-doped ZnO ceramics. *J Europ Ceram Soc.* 2002;22:1653–60. [https://doi.org/10.1016/S0955-2219\(01\)00484-8](https://doi.org/10.1016/S0955-2219(01)00484-8).
2. A. Boumezoued, K. Guergouri, M. Zaabat, D. Recham, R. Barille, Investigation of structural and electrical properties of manganese doped ZnO varistors prepared from nanopowders. In: Proceedings of international agricultural, biological & life science conference, Sept 2–5, Edirne, Turkey; 2018. p. 250–258.
3. Singhal RK, Dhawan MS, Gaur SK, Dolia SN, Kumar S, Shripathi T, Deshpande UP, Xing YT, Saitovitch E, Garg KB. Study of ferromagnetism in Mn doped ZnO dilute semiconductor system. *J Phys Conf Ser.* 2009;153:012065. <https://doi.org/10.1088/1742-6596/153/1/012065>.
4. Shatnawi M, Alsmadi AM, Bsoul I, Salameh B, Mathai M, Alnawashi G, Alzoubi GM, Al-Dweri F, Bawa'aneh MS. Influence of Mn doping on the magnetic and optical properties of ZnO nanocrystalline particles. *Results Phys.* 2016;6:1064–71. <https://doi.org/10.1016/j.rinp.2016.11.041>.
5. Liu W, Tang X, Tang Z. Effect of oxygen defects on ferromagnetism of Mn doped ZnO. *J Appl Phys.* 2013;114(12):123911. <https://doi.org/10.1063/1.4823774>.
6. Luo X, Lee W-T, Xing G, Bao N, Yonis A, Chu D, Lee J, Ding J, Li S, Yi J. Ferromagnetic ordering in Mn-doped ZnO nanoparticles. *Nanoscale Res Lett.* 2014;9:625. <https://doi.org/10.1186/1556-276X-9-625>.
7. Ali N, Singh B, Vijaya AR, Lal S, Yadav CS, Tarafder K, Ghosh S. Ferromagnetism in Mn-doped ZnO: a joint theoretical and experimental study. *J Phys Chem C.* 2021;125(14):7734–45. <https://doi.org/10.1021/acs.jpcc.0c08407>.
8. Korsunskaya NO, Borkovskaya LV, Bulakh BM, Khomenkova LY, Kushnirenko VI, Markevich IV. The influence of defect drift in external electric field on green luminescence of ZnO single crystals. *J Lumin.* 2003;102–103:733–6. [https://doi.org/10.1016/S0022-2313\(02\)00634-8](https://doi.org/10.1016/S0022-2313(02)00634-8).
9. Markevich IV, Kushnirenko VI, Borkovskaya LV, Bulakh BM. Mechanism of formation of highly conductive layer on ZnO crystal surface. *Solid State Commun.* 2005;136(8):475–8. <https://doi.org/10.1016/j.ssc.2005.09.001>.
10. Borkovskaya LV, Bulakh BM, Kushnirenko VI, Markevich IV, Rusavsky AV. Influence of dislocation decoration with mobile donors on exciton luminescence in ZnO crystals. *Phys Stat Sol (C).* 2007;4(8):3086–9. <https://doi.org/10.1002/pssc.200675473>.
11. Das PP, Samanta S, Wang L, Kim J, Vogt T, Sujatha Devi P, Lee Y. Redistribution of native defects and photoconductivity in ZnO under pressure. *RSC Adv.* 2019;9:4303–13. <https://doi.org/10.1039/C8RA10219H>.
12. Gupta TK, Mathur MP, Carlson WG. Effect of externally applied pressure on zinc oxide varistors. *J Electron Mater.* 1977;6:483–97. <https://doi.org/10.1007/BF02672229>.
13. Dorlanne O, Ai B, Destruel P, Loubiere A. Electrical characteristics of zinc oxide varistors subjected to hydrostatic pressure. *J Appl Phys.* 1985;57:5535–8. <https://doi.org/10.1063/1.334834>.
14. Schoutens JE, Senesac SL. Effect of hydrostatic pressure up to 25 kbars on zinc oxide varistors: static loading. *J Appl Phys.* 1979;50:6283–9. <https://doi.org/10.1063/1.325767>.
15. Raidl N, Hofstatter M, Supancic P. Piezotronic effect on electrical characteristics of bulk ZnO varistors. *Adv Eng Mater.* 2016;19:201600677. <https://doi.org/10.1002/adem.201600677>.
16. Korsunskaya N, Markevich I, Ponomaryov S, Polishchuk Y, Tsybrii Z, Khmil D, Stara T, Melnichuk O, Melnichuk L, Venger Y, Kladko V, Khomenkova L. Effect of milling of ZnO and MgO powders on structural, optical, and electrical properties of (Mg, Zn)O ceramics. *Phys Stat Sol (A).* 2022;219:2200050. <https://doi.org/10.1002/pssa.202200050>.
17. Borkovskaya LV, Kushnirenko VI, Markevich IV, Khomenkova LY. Residual donors in zinc oxide: nature and influence on the properties of crystals. *Optoelectron Semicond Tech.* 2005;40:179–89 (in Russian).
18. Markevich IV, Kushnirenko VI, Borkovskaya LV, Bulakh BM. Mobile donors in undoped ZnO. *Phys Status Solidi (C).* 2006;3:942–5. <https://doi.org/10.1002/pssc.200564757>.
19. Ohashi N, Terada Y, Ohgaki T, Tsurumi T, Fukunaga O, Hanega H, Tanaka J. Synthesis of ZnO bicrystals doped with Co or Mn and their electrical properties. *Jpn J Appl Phys.* 1999;38:5028–32. <https://doi.org/10.1143/JJAP.38.5028>.
20. Markevich I, Stara T, Vorona I, Isaieva O, Gule Y, Melnichuk O, Khomenkova L. Role of ZnMn₂O₄ phase in the formation of varistor characteristics in ZnO:Mn ceramics. *Semicond Phys Quantum Electron Optoelectron.* 2023;26(3):255–9. <https://doi.org/10.15407/spqeo26.03.255>.
21. Oba F, Nishitani SR, Adachi H, Tanaka I, Kohyama M, Tanaka S. Ab initio study of symmetric tilt boundaries in ZnO. *Phys Rev B.* 2001;63:045410. <https://doi.org/10.1103/PhysRevB.63.045410>.
22. Markevich IV, Kushnirenko VI, Rusavsky AV. Influence of boric acid as a flux on the properties of ZnO ceramics. *Rad Meas.* 2010;45:468–71. <https://doi.org/10.1016/j.radmeas.2009.12.015>.
23. Venger EF, Melnichuk AV, Melnichuk LJ, Pasechnik JA. Anisotropy of the ZnO single crystal reflectivity in the region of residual rays. *Phys Status Solidi B.* 1995;188:823–31. <https://doi.org/10.1002/pssb.2221880226>.
24. Melnichuk O, Melnichuk L, Venger E. Phonon and Plasmon-phonon interactions in ZnO single crystals and thin films. In: Savkina R, Khomenkova L, editors. *Oxide-based materials and structures.* Boca Raton: CRC Press; 2020. p. 163–200.
25. Melnichuk OV, Korsunskaya NO, Markevich IV, Boyko VV, Polishchuk YO, Tsybrii ZF, Melnichuk LY, Venger YF, Kladko VP, Khomenkova LY. Peculiarities of specular infrared reflection spectra of ZnO-based ceramics. *Semicond Phys Quantum Electron Optoelectron.* 2021;24(4):390–8. <https://doi.org/10.15407/spqeo24.04.39>.
26. Piqueras J, Kubalek E. Cathodoluminescence from deformed ZnO ceramics. *Sol State Commun.* 1985;54:745–6. [https://doi.org/10.1016/0038-1098\(85\)90601-5](https://doi.org/10.1016/0038-1098(85)90601-5).

Publisher's Note Springer Nature remains neutral with regard to jurisdictional claims in published maps and institutional affiliations.